

Article

Structural Stability and Performance of Noble Metal-Free SnO₂-Based Gas Sensors

Antonio Tricoli

Department of Mechanical and Process Engineering, ETH Zurich, CH-8092 Zurich, Switzerland;
E-Mail: atricoli@ethz.ch; Tel.: +41-44-632-8503; Fax: +41-44-632-1276

Received: 22 April 2012; in revised form: 18 May 2012 / Accepted: 25 May 2012 /

Published: 29 May 2012

Abstract: The structural stability of pure SnO₂ nanoparticles and highly sensitive SnO₂-SiO₂ nanocomposites (0–15 SiO₂ wt%) has been investigated for conditions relevant to their utilization as chemoresistive gas sensors. Thermal stabilization by SiO₂ co-synthesis has been investigated at up to 600 °C determining regimes of crystal size stability as a function of SiO₂-content. For operation up to 400 °C, thermally stable crystal sizes of *ca.* 24 and 11 nm were identified for SnO₂ nanoparticles and 1.4 wt% SnO₂-SiO₂ nanocomposites, respectively. The effect of crystal growth during operation ($T_0 = 320$ °C) on the sensor response to ethanol has been reported, revealing possible long-term destabilization mechanisms. In particular, crystal growth and sintering-neck formation were discussed with respect to their potential to change the sensor response and calibration. Furthermore, the effect of SiO₂ cosynthesis on the cross-sensitivity to humidity of these noble metal-free SnO₂-based gas sensors was assessed.

Keywords: gas sensors; SnO₂; semiconductors; chemoresistive; nanoparticles; long-term stability; grain growth; relative humidity; noble metals; SiO₂

1. Introduction

Metal-oxide nanoparticles of a few nanometers such as SnO₂ are excellent materials for the fabrication of solid-state gas sensors [1]. Highly porous film morphologies constituted by such nanoparticles have remarkable potential for several novel and demanding applications such as non-invasive medical diagnostics [2]. However, small nanoparticles suffer from poor thermal stability resulting in insufficient long-term stability of the sensing properties (e.g., baseline and calibration

drifts) already at standard operation temperatures (250–500 °C) [3]. Utilization of large particles allow synthesis of thermally more stable film structures with, however, considerably lower sensitivity [4]. In fact, the sensitivity of SnO₂ nanoparticles increases drastically with decreasing grain size toward twice their Debye length (*ca.* 6 nm at 300 °C) [4,5]. Furthermore, small variation of the neck size between large particles is possible during operation and may also result in a drift of the sensing properties.

Often, addition of noble metals (Ag and Pt) is utilized to enhance the sensitivity of large SnO₂ grains by the spill-over effect [6]. However, clustering and growth of the noble metal on the metal-oxide surface during sensor operation is in itself a potential long-term destabilization mechanism [3]. Additionally, deposition of noble metals on the metal-oxide surface increases material cost and process complexity. Noble metal-free enhancement of the sensitivity of SnO₂ nanoparticles has been achieved, recently, by flame-cosynthesis of SiO₂ [7]. Optimized SnO₂-SiO₂ nanocomposites have demonstrated both drastically higher sensor response and short-term thermal stability [7].

The long-term stability of these nanocomposites and the effect of SiO₂ cosynthesis on other important sensors properties such as the cross-sensitivity to humidity have not been investigated so far [7–9]. Deposition of flame-made SiO₂ led to the synthesis of super-hydrophilic surfaces suggesting that its cosynthesis may increase the cross-sensitivity of SnO₂-based gas sensors to humidity [10,11]. Furthermore, flame-synthesis of SiO₂ at low precursor concentration has shown that SiO₂ does not nucleate as easily as other oxides (e.g., SnO₂ and TiO₂) [9,11] and thus may condense directly on the surface of the SnO₂ nanoparticles. Surface localized SiO₂ could act as active center for the adsorption of H₂O molecules. This would limit the utilization of SnO₂-SiO₂ nanocomposites to constant humidity applications and may even result in a drastic drop of their sensing performance [9].

The long-term stability of nanoparticles is dependent on their grain size and sintering/operation temperature [3,12]. Although, SiO₂ cosynthesis has demonstrated to drastically decrease sintering rates [7], the thermodynamically stable crystal and grain sizes of SnO₂-SiO₂ nanocomposites have not been determined. In particular, films made of fine nanoparticles may require a very long time to reach sufficient structural stability [12] causing a continuous drift of their electronic properties [3]. The thermal stabilization mechanism of SiO₂ also plays an important role in the resulting sensor performance dynamics and requires further investigation [7,13,14].

Here, we investigate the long-term structural stability of flame-made SnO₂-SiO₂ nanocomposites focusing on the electronic properties of the resulting sensing films. Temperature-dependent thermally stable sizes are identified for pure SnO₂ nanoparticles and tailored SnO₂-SiO₂ nanocomposites. The effect of crystal growth during sensor operation is investigated and discussed with respect to possible long-term instability mechanisms. Furthermore, the effect of SiO₂ cosynthesis on the cross-sensitivity to humidity of the resulting gas sensors is critically compared to that of pure SnO₂.

2. Experimental Section

Pure SnO₂ nanoparticles with 12 and 21 ± 0.5 nm average crystal size (d_{XRD}) and tailored SnO₂-SiO₂ nanocomposites were produced by flame spray pyrolysis (FSP) as previously described [7,15]. In particular, the deposition time was 4 min for all sensors and was followed by a 30 s *in situ* annealing step at 14 cm HAB with a particle-free xylene flame (12 mL/min) leading to a film bulk thickness of *ca.* 0.8 μm. It is expected that SiO₂ formation may slightly increase the visible film thickness due to its

lower density and by inhibiting SnO₂ grain sintering. During deposition the substrate back temperature was 120–130 °C as measured by a n-type thermocouple. Furthermore, nanoparticles were collected on water cooled glass-fiber filters placed at 50 cm height above the burner (HAB) and characterized by transmission electron microscopy (TEM) with a Hitachi H600 microscope, operated at 100 kV. X-ray diffraction (XRD) patterns were obtained by a Bruker, AXS D8 Advance diffractometer operated at 40 kV, 40 mA at 2θ (Cu Kα) = 15–75°, step = 0.03 and scan speed = 0.6°/min. The d_{XRD} was determined using the Rietveld fundamental parameter method with the structural parameters of cassiterite [16]. Sintering studies were performed by placing the nanoparticles in a furnace (Carbolite) in air under atmospheric pressure.

The nanoparticle specific surface area (SSA) was measured by BET analysis using a Micromeritics Tristar 3000. The BET equivalent diameter (d_{BET}) was calculated using the density of SnO₂ and SiO₂. Sensing films were obtained by direct impingement of the FSP aerosol and *in situ* flame annealing on alumina substrates with Au interdigitated electrodes as previously described [7,15]. The sensor measurements were performed as described in detail elsewhere [17]. The analyte mixture was EtOH (105 ppm ± 3% synthetic air, Pan Gas 5.0) in synthetic air (20.8% ± 2% O₂ rest nitrogen, Pan Gas 5.0). Water vapor was supplied by an air flow let through a bubbler kept at 20 °C. The temperature was measured with a n-type thermocouple [17]. The sensor response (S) was defined as in Equation (1) [18]:

$$S = \frac{R_{air}}{R_{EtOH}} - 1 \quad (1)$$

where R_{air} is the film resistance in air with a given relative humidity (r.h.) and R_{EtOH} is the film resistance with a given concentration of ethanol at the same r.h.. The cross-sensitivity (CS) to humidity was defined as [9]:

$$CS = abs \left[\frac{S_{dry} - S_{\%r.h.}}{S_{dry}} \right] \cdot 100 \quad (2)$$

where S_{dry} is the response in dry air and S_{%r.h.} is the response at a given r.h. as defined in Equation (1).

3. Results and Discussion

3.1. Long-Term Structural Stability of SnO₂-SiO₂ Nanocomposites

Crystal growth during operation at the elevated working-temperatures (250–500 °C) of metal-oxide gas sensors is considered to contribute to the drift of their baseline (film resistance without the analyte) and poor long-term stability of their response [2,3]. The BET and XRD size were within 1 nm suggesting formation of mainly monocrystalline particles. Figure 1 shows the average crystal size of large (triangles) and small (squares) SnO₂ nanoparticles as a function of the sintering time at 400 °C. The crystal size of the better performing, small SnO₂ nanoparticles (Figure 1, squares) increased from 12 to 22 nm with increasing sintering time from 0 to 24 h. A crystal size of 21.6 nm was obtained already after 12 h sintering (Figure 1, squares). In contrast, the crystal size of the large SnO₂ nanoparticles (Figure 1, triangles) increased only from 21.9 to 24.2 with increasing sintering time from 0 to 24 h. This indicates that, for sensor operation at 400 °C, flame-made nanoparticles constituted by pure SnO₂ crystals have a thermodynamically stable size of nearly 24 nm in agreement with the poor

thermal stability of small SnO₂ nanoparticles and with the grain size stability conditions reported for several other synthesis methods [3]. This is in line with the rapid crystal and grain growth of flame-made SnO₂ nanoparticles observed already at low sintering temperatures [7] suggesting that obtaining stable sensor responses requires testing of the sensors for several consecutive days. In particular, the asymptotic-like growth of the small SnO₂ nanoparticles (Figure 1, squares) toward 22 nm suggests that small drift of sensor response and baseline may continue for a very long time span (>>24 h). In fact, the thermodynamically stable crystal size (at 400 °C) of 24 nm was still not obtained upon 24 h sintering.

Figure 1. Average crystal size (d_{XRD}) of large (triangles) and small (squares) SnO₂ nanoparticles as a function of the sintering time at 400 °C. Cosynthesis of 1.4 wt% SiO₂ (circles) drastically increased the long-term thermal-stability of SnO₂ crystals.

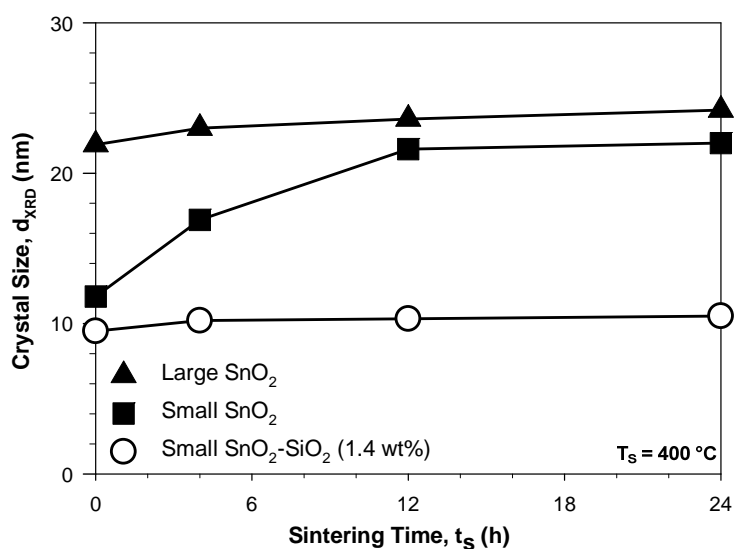
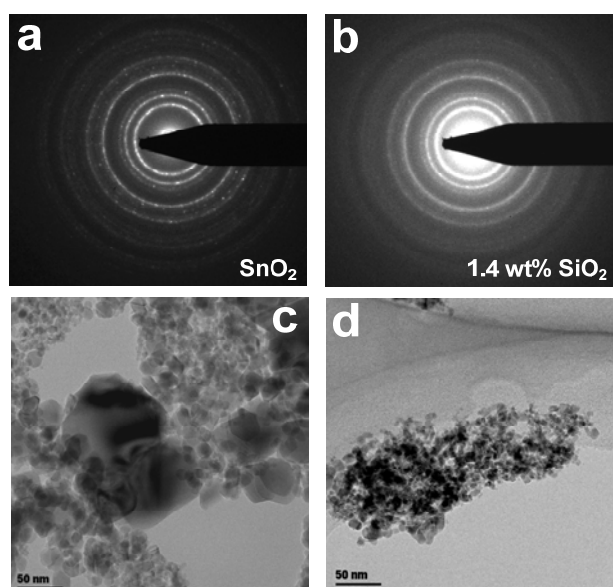


Figure 2. ED patterns of pure (a) SnO₂ nanoparticles and (b) 1.4 wt% SnO₂-SiO₂ nanocomposites after 4 h sintering at 400 °C and corresponding transmission electron microscopy (TEM) images (c,d).



Cosynthesis of SiO_2 led already at very low content (1.4 wt%) to remarkable long-term thermal-stabilization of the small SnO_2 nanoparticles. The average crystal size of these SnO_2 - SiO_2 nanocomposites (Figure 1, circles) increased only from 9.5 to 10.5 nm with increasing sintering time from 0 to 24 h. The particles were mainly polyhedral (Figure 2(c,d)) consisting of a crystalline SnO_2 core and some dispersed SiO_2 phase. At high SiO_2 content, the SnO_2 and SiO_2 phase were segregated in crystalline and amorphous domains, respectively. This is in line with the reported thermal stabilization and performance maximization of SnO_2 - [7] and WO_3 -based [19] gas sensors by Si-doping. Here, it is shown that this noble metal-free approach to improve the performance of metal-oxide chemoresistive gas sensors offers also superior long-term structural stability.

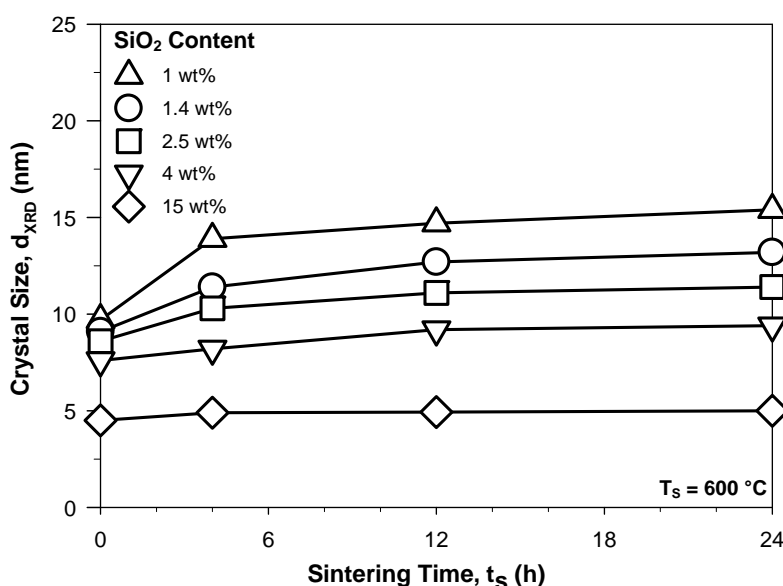
The thermal stabilization mechanism of the small SnO_2 crystals by SiO_2 cosynthesis was further investigated by electron diffraction analysis, XRD and TEM analysis of the nanoparticles upon sintering for 4 h at 400 °C. In line with previous results [7], increasing the SiO_2 content increased the homogeneity of the visible SnO_2 TEM size both for the as-prepared and sintered samples. The electron diffraction (ED) patterns of the small SnO_2 nanoparticles (Figure 2(a)) showed the presence of crystalline structures in line with the XRD analysis [7] that corresponded to 100 wt% cassiterite phase [16] while the numerous bright spots indicate the formation of large crystals already upon short (4 h) sintering at 400 °C. This is in line with the rapid increase in average crystal size of the small SnO_2 nanoparticles (Figure 1, squares) with increasing sintering time and suggests a polydisperse crystal size distribution. In contrast, the ED patterns of the 1.4 wt% SnO_2 - SiO_2 nanocomposites (Figure 2(b)) did not show nearly any bright spot. This indicates that the formation of large crystals is homogeneously inhibited by cosynthesis of SiO_2 . In this respect, a possible thermal stabilization mechanism is the pinning of the SnO_2 crystal boundaries by SiO_2 [13,14]. Condensation of the SiO_2 molecules on the surface of the nucleated SnO_2 clusters during flame-synthesis may explain the lower sintering rates of these SnO_2 - SiO_2 nanoparticles already at very low SiO_2 content. In fact, it is expected that SiO_2 segregates from the SnO_2 already at low content (*ca.* 2 wt%) [7].

This homogeneous inhibition of SnO_2 crystal growth is necessary to achieve long-term stability of the sensing properties. In fact, irregular growth of some un-stabilized SnO_2 nanoparticles would also lead to change in the structural and electronic properties of the sensing film. However, the crystal size of the SnO_2 - SiO_2 nanocomposites (Figure 1, circles) was not completely stable and approached slowly 10.5 nm. Although, this crystal growth is very small with respect to that of pure SnO_2 (Figure 1, squares), it still indicates a restructuring of the nanoparticle interface. In particular, growth of sintering necks may drastically change the performance of the sensing film while showing very small variations in the measured crystal size [7].

Reduction of the long-term drift of the SnO_2 and SnO_2 - SiO_2 sensors may be obtained by pre-sintering of the films at temperatures above the operational ones (e.g., at 600 °C) [7] leading to the achievement of a thermodynamically stable grain size prior to sensor testing (e.g., at 400 °C). Figure 3 shows the average SnO_2 crystal size of several SnO_2 - SiO_2 nanocomposites as a function of such a pre-sintering step at 600 °C. The 1 wt% SnO_2 - SiO_2 crystal size (Figure 3, triangles up) increased from 9.7 to 15.4 nm with increasing sintering time at 600 °C from 0 to 24 h. This shows that even the smallest addition of SiO_2 leads to stabilization of the SnO_2 crystal size far below that of pure SnO_2 at 400 °C (Figure 1, solid triangles). In particular, the 1.4 wt% SnO_2 - SiO_2 reached a size of 11.4 nm already after 4 h sintering (Figure 3, circles). This is more than the thermodynamically stable size

(≈ 10.5 nm) at 400 °C and thus pre-sintering of the sensing films prior to sensor utilization may be utilized to considerably shorten the time required for achievement of a stable sensor response. Furthermore, up to 4 wt% SiO₂, the as-prepared SnO₂ crystal size (Figure 3) of these nanocomposites was very close (*ca.* 10 \pm 1.5 nm) suggesting further that SiO₂ may condense directly on the formed SnO₂ nanoparticles inhibiting further crystal and grain growth during flame-synthesis. In comparison, the initial crystal size of the pure SnO₂ nanoparticles was 12 nm (Figure 1, solid squares) which is attributed to particle coagulation during the residence time in the flame. In line, the as-prepared powder SSA increased from 100 to 211 m²/g with increasing SiO₂ content from 0 to 15 wt%. The 15 wt% SiO₂-SnO₂ demonstrated the highest long-term stability growing only from 4.5 to 5 nm (Figure 3, diamonds) with increasing sintering time from 0 to 24 h. This is in agreement with the grain growth inhibition demonstrated by SiO₂ cosynthesis [7]. However, utilization of such high SiO₂ contents results in the formation of insulating domains and a drastic drop of the sensing performance [7] and thus, here, the dynamics of the sensor response stabilization has been investigated at low SiO₂ content (1–4 wt%).

Figure 3. Average SnO₂ crystal size (d_{XRD}) of the SnO₂-SiO₂ nanocomposites as a function of the sintering time at 600 °C for several SiO₂ contents.



3.2. Sensing Performance Stability

The sensing properties of these SnO₂-SiO₂ nanoparticles were tested with EtOH, a standard volatile organic compound that is particularly important for detection of drunken drivers and is increasingly investigated also for non-invasive breath analysis. Figure 4 shows the response to 10 ppm ethanol of a pure SnO₂ ($d_{\text{XRD}} = 12$ nm) gas sensor, that was not stabilized by a pre-sintering step, for several operation temperatures. The response of this sensor (Figure 4) decreased considerably with increasing operation temperature from 220 to 320 °C. This is surprising as pure SnO₂ has maximal response to EtOH at around 300–350 °C [20]. The drop in the sensor response was attributed to the sintering of the SnO₂ nanoparticles already during operation at such moderate temperatures. This is in line with the measured crystal growth of the small SnO₂ nanoparticles (Figure 1, solid squares) that is expected to

drastically reduce their sensitivity [3,5,7]. Additionally, operation of the SnO₂ sensor at 220 °C was characterized (Figure 4, dotted line) by an unstable response and it was not possible to fully recover the initial baseline. This indicates that without prior stabilization the sensing behavior of pure SnO₂ nanoparticles is characterized by very poor long-term stability. After two days at 320 °C (Figure 4, solid line), the sensor properties were considerably more stable demonstrating a well-defined response to 10 ppm EtOH and full recovery of the initial baseline. Nevertheless, increasing the EtOH concentration to 30 and 50 ppm (Figure 5) resulted in very long response times.

Figure 4. Response of a gas sensor made of as prepared SnO₂ nanoparticles ($d_{\text{XRD}} = 12 \text{ nm}$) to 10 ppm ethanol as a function of time for increasing operation temperature from 220 to 320 °C.

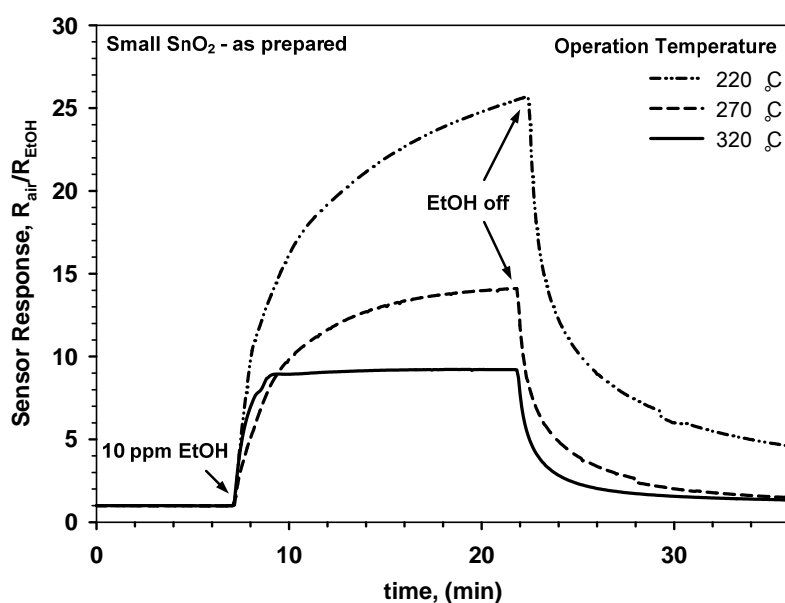
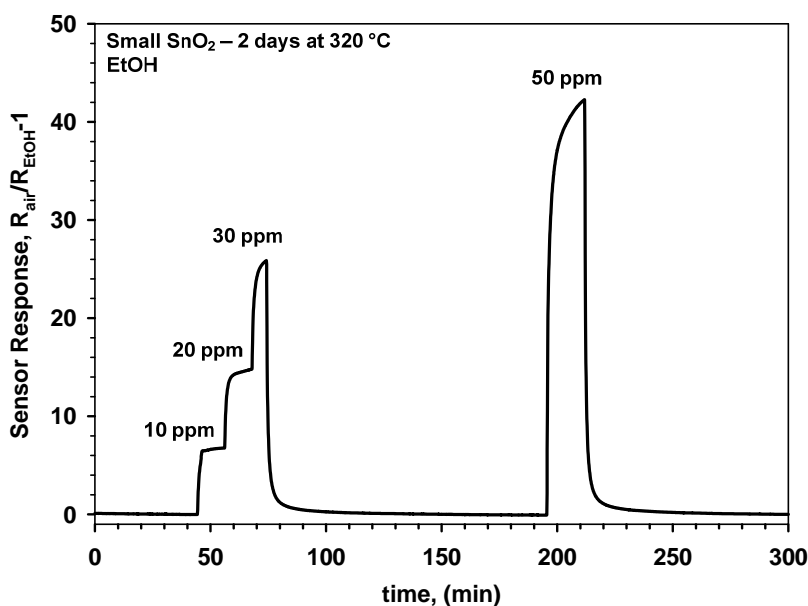


Figure 5. Response of a gas sensor made of small SnO₂ nanocrystals to ethanol without prior stabilization upon two days at 320 °C in dry air.



The step-wise increase of the EtOH concentration (Figure 5) from 10 to 30 ppm at 320 °C demonstrated sufficient sensor sensitivity for discerning among small (<10 ppm) EtOH variations. Furthermore, a very good recovery of the initial baseline was observed (Figure 5) in line with the single EtOH step at 320 °C (Figure 4, solid line). However, the sensitivity of this SnO₂ sensor to EtOH was pretty low with respect to noble-metals [6] or metal-oxide [7] doped nanoparticles. This was also attributed to the growth of the SnO₂ crystals during operation and that was found to undermine the reproducibility of the sensor performance. To have more stable sensing properties, novel sensors made of pure SnO₂ nanoparticles ($d_{\text{XRD}} = 12$ nm) were also tested for EtOH sensing after a sintering step at 600 °C (12 h). Their performance was compared to the sensors (Figures 4 and 5) with the as prepared nanoparticle films.

Figure 6. Response of a gas sensor made of small SnO₂ nanocrystals to ethanol after a 12 h sintering step at 600 °C.

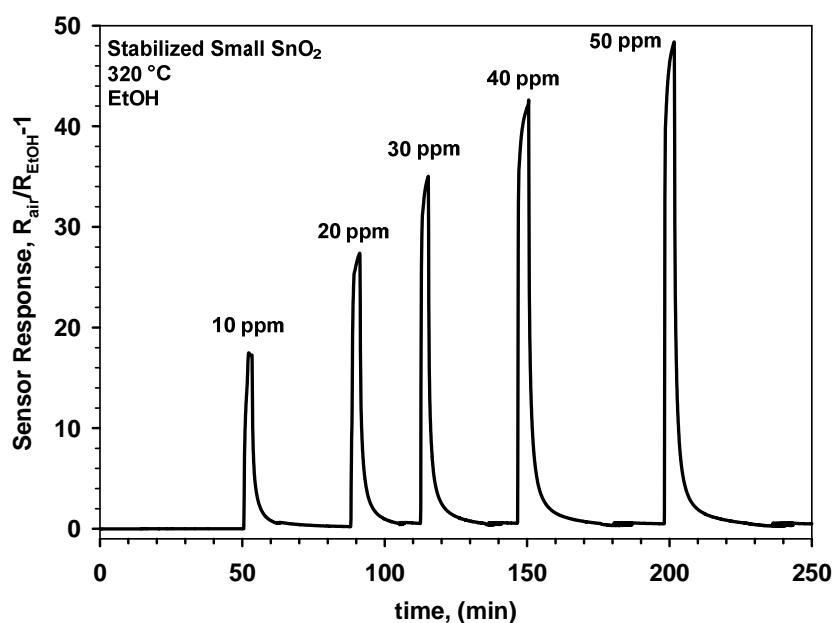
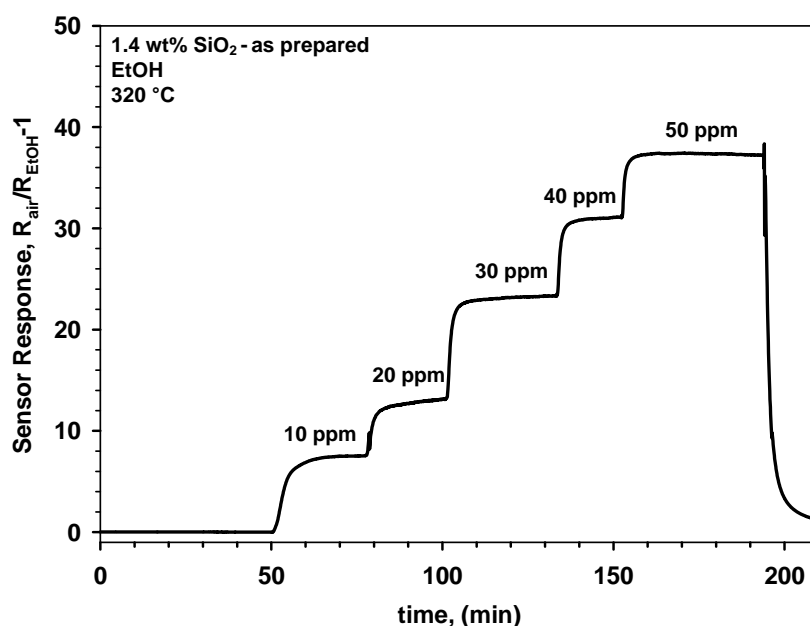


Figure 6 shows the response to increasing EtOH concentrations of a SnO₂ sensor made of small nanoparticles that was sintered at 600 °C for 12 h prior to gas sensing. The sensor shows (Figure 6) similar response and recovery time to that having an as prepared SnO₂ nanoparticle film (Figure 5). This is in agreement with the identical surface composition and film thickness of the as prepared and sintered SnO₂ films. However, the magnitude of the sensor response was drastically increased with respect to the latter. In particular, the sintered sensor (Figure 6) had a response of nearly 17 to 10 ppm of EtOH while the as prepared barely reached 8. This is surprising as high temperature sintering is expected to increase crystal size leading to lower sensitivity [3,5]. Here, it is suggested that the enhancement of the sensor response arise from the formation of sintering necks with size below that of the main grains between the SnO₂ particles. Formation of partially or fully depleted sintering necks can increase the sensitivity of metal-oxide gas sensors and can hardly be measured by XRD or nitrogen adsorption [7]. As a result, two instability mechanisms are suggested for the pure SnO₂ nanoparticles. A first, where the average crystal (and grain) size is increased (Figure 4) resulting in a drop of the sensor response, and a second, where partially depleted sintering necks are formed increasing the

sensitivity. Similar effects were observed for size selected SnO₂ agglomerates [21]. There, very small changes in the sintering properties of the agglomerates that could hardly be tracked by XRD analysis led to drastic variations in their sensing response to EtOH. Both dynamics can be accelerated by a pre-sintering step leading to (Figure 6) higher response and more stable sensing properties.

The sensing dynamics of the SnO₂-SiO₂ composites was different from that of the pure SnO₂ nanoparticles (Figures 4–6). To better investigate the effect of SiO₂ cosynthesis on the sensing properties, all synthesis parameters were kept constant and only the Si-content was varied. Figure 7 shows the response to step-wise increases in EtOH concentration of a sensor made of as prepared 1.4 wt% SnO₂-SiO₂. The response and recovery times of these nanocomposites (Figure 7) were comparable to that of the pure SnO₂ (Figure 5). Nevertheless, the magnitude of the sensor response was initially lower than that of the SnO₂ nanoparticles (Figure 5) reaching about 37 at 50 ppm EtOH (Figure 7). This is in contrast to the smaller crystal size of these nanocomposites (Figure 3, triangles up) that should lead to higher sensitivity [5]. This is attributed to the sintering inhibition effect of the SiO₂ that may have limited the growth of sintering neck between the main SnO₂ grains.

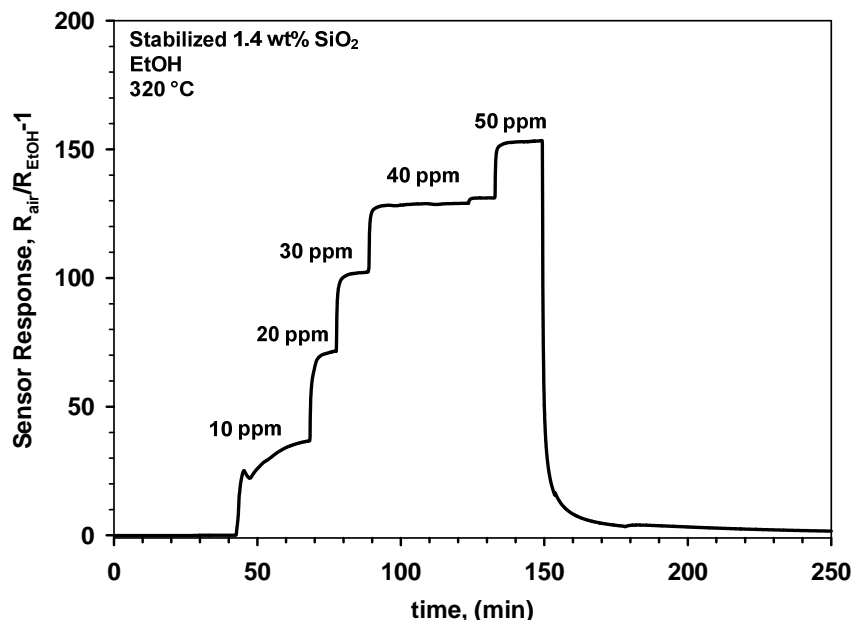
Figure 7. Response of a gas sensor made of as prepared 1.4 wt% SnO₂-SiO₂ nanocomposites to increasing EtOH concentrations in dry air.



After sintering these films at 600 °C for 12 h, their response was greatly increased (Figure 8). More in details, upon this stabilization step, the response of the 1.4 wt% SnO₂-SiO₂ to 50 ppm EtOH increased from 37 (Figure 7) to 153 (Figure 8). This 4 fold increase in sensitivity is in line with the reported optimal Si-doping of SnO₂ nanoparticles [7]. Furthermore, it confirms the long-term instability mechanisms observed for pure SnO₂. As the presence of SiO₂ drastically inhibit the crystal growth, the sintering necks formed at 600 °C are smaller and thus more depleted than for pure SnO₂ (Figures 5 and 6) resulting in a more drastic enhancement of their sensing performance (Figures 7 and 8). A more detailed analysis of the neck morphologies and growth dynamics is required to quantitatively describe the sensing response enhancement of these nanocomposites [4]. Higher SiO₂ contents (Figure 3), up to 4 wt%, resulted in a similar enhancement of the sensing properties. Overall, cosynthesis

of SiO₂ increases the variation of sensor resistance during injection of EtOH concentration as it was previously investigated in details [7].

Figure 8. Response to increasing EtOH concentrations in dry air of a gas sensor made of 1.4 wt% SnO₂-SiO₂ nanocomposites upon stabilization by sintering for 12 h at 600 °C.

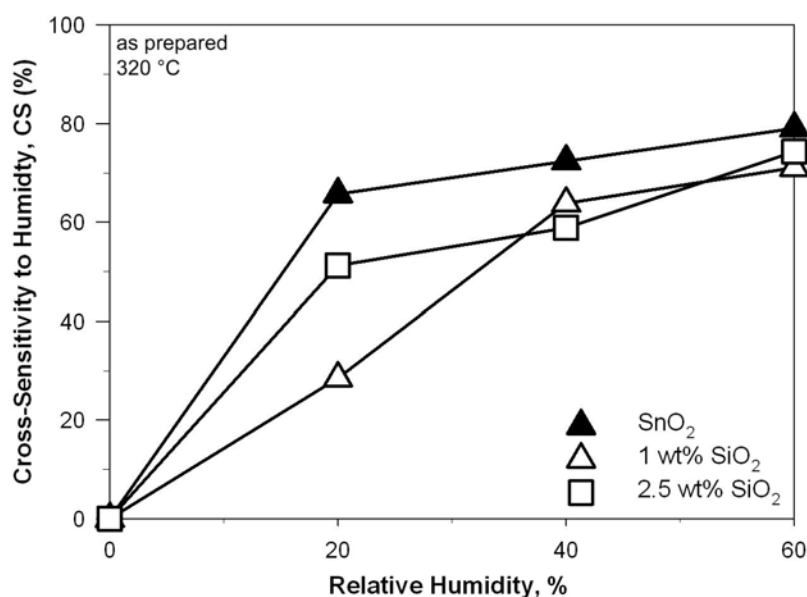


3.3. Cross-Sensitivity to Humidity

The stability of the sensor response toward variations in relative humidity is of major importance for several applications [2,22]. Doping of SnO₂ nanoparticles with Ti has been reported to drastically decrease their cross-sensitivity to humidity [9]. Recently, this has been attributed to thermodynamically dictated enrichment of the SnO₂ surface with Ti atoms [23] that lower the adsorption energy of dissociatively adsorbed H₂O [24]. The effect of SiO₂ cosynthesis on the cross-sensitivity (CS) to humidity of SnO₂ nanoparticles, however, has not been investigated yet. This is particularly important as flame-made SiO₂ has high surface concentration of hydroxyl groups that facilitate the binding of H₂O molecules [10] and thus may result in a strong enhancement of the CS to humidity. Figure 9 shows the CS to humidity during EtOH detection, defined as change of the sensor response in dry air (Equation (2)), of the pure SnO₂ (triangles solid), 1 wt% (empty triangles) and 2.5 wt% (empty squares) SnO₂-SiO₂ nanocomposites as a function of the relative humidity. The CS to humidity of the pure SnO₂ sensors (Figure 9, solid triangles) increased from 51 to 74% with increasing r.h. from 20 to 60%. This is in agreement with the drastic change in sensor response reported for SnO₂ nanoparticles with increasing r.h. content [9]. The continuous increase in CS above 20% r.h. (Figure 9, solid triangles) indicates that the SnO₂ surface has not yet been saturated with adsorbed H₂O species. More important, the CS of both SnO₂-SiO₂ sensors (Figure 9, empty squares and triangles) was comparable to that of the pure SnO₂ (Figure 9, solid triangles). This is different than the effect of Ti-doping [7] and in contrast to the super-hydrophilic properties of flame-made SiO₂ [10]. However, as SiO₂ is an isolator, localized SiO₂ molecules/clusters on the SnO₂ surface may act as active sites for H₂O binding but still have minimal impact on the sensing properties of the SnO₂ nanocrystals due to its inefficient

electron conduction properties. As a result, SiO₂ cosynthesis leads to the same CS than pure SnO₂ nanoparticles. This is in contrast to the modification of SnO₂ crystals with hydrophilic zeolites [25,26] where notable variations from the sensing response of the pure SnO₂ were observed. Minimization of the CS while improving the long-term stability and sensitivity of SnO₂-based gas sensors may be achieved by synthesis of Sn_{1-x}Ti_xO₂-SiO₂ nanocomposites [9].

Figure 9. Cross-sensitivity to relative humidity (20 °C) of as prepared SnO₂ nanoparticles (solid triangles), and of 1 wt% (empty triangles) and 2.5 wt% (squares) SnO₂-SiO₂ nanocomposites at 320 °C.



It should be pointed out that the sensing chamber geometry has considerable influence on the resulting sensor response dynamics as previously discussed in details [27]. The setup utilized here was previously tested for several other materials [7,9,15,17] and, for the utilized total gas flow (1 L/min), results in reaction limited sensor responses [27].

4. Conclusions

The long-term structural stability of small SnO₂ nanoparticles has been investigated for temperatures relevant to metal-oxide gas sensor operation. A stable SnO₂ crystal size of *ca.* 24 nm has been determined for operation at up to 400 °C. This stable size was decreased to *ca.* 11 nm by cosynthesis of 1.4 wt% SiO₂. However, the slow asymptotic-like growth of the SnO₂ crystals indicated poor long-term stability even for such thermodynamically more stable nanocomposites. This was further confirmed by investigation of the sensing response of the as prepared SnO₂ nanoparticle sensors. Two main instability mechanisms were suggested: first a response drop due to crystal growth and then a response enhancement due to the formation of full or partially depleted sintering necks. Analysis of the performance of SnO₂-SiO₂ nanocomposites confirmed that sintering the films at 600 °C for 12 h prior gas sensing increases sensor stability and performance. Furthermore, the effect of SiO₂ cosynthesis on the cross-sensitivity to humidity of SnO₂-based gas sensors was investigated. Cosynthesis of up to 2.5 wt% SiO₂ had no effect on the sensor cross-sensitivity to humidity suggesting

minimal electronic interaction between SnO₂ and SiO₂. These results show that SnO₂-SiO₂ nanocomposites can enhance the long-term stability and sensitivity of SnO₂-based gas sensors while having minimal impact on the residual SnO₂ properties.

Acknowledgments

The author is thankful to M. Righettoni (ETH Zurich) for the help with the characterization of the SnO₂-SiO₂ nanocomposites, to F. Krumeich (EMEZ, ETH Zurich) for electron microscope analysis, and to S.E. Pratsinis (ETH Zurich) and P. Gouma (SUNY) for fruitful discussions. Financial support was provided by CCMX and NANOPRIM.

References

1. Eranna, G.; Joshi, B.C.; Runthala, D.P.; Gupta, R.P. Oxide materials for development of integrated gas sensors—A comprehensive review. *Crit. Rev. Solid State Mater. Sci.* **2004**, *29*, 111–188.
2. Tricoli, A.; Righettoni, M.; Teleki, A. Semiconductor gas sensors: Dry synthesis and application. *Angew. Chem. Inter. Ed.* **2010**, *49*, 7632–7659.
3. Korotcenkov, G. Gas response control through structural and chemical modification of metal oxide films: State of the art and approaches. *Sens. Actuat. B Chem.* **2005**, *107*, 209–232.
4. Rothschild, A.; Komem, Y. The effect of grain size on the sensitivity of nanocrystalline metal-oxide gas sensors. *J. Appl. Phys.* **2004**, *95*, 6374–6380.
5. Ogawa, H.; Nishikawa, M.; Abe, A. Hall measurement studies and an electrical-conduction model of tin oxide ultrafine particle films. *J. Appl. Phys.* **1982**, *53*, 4448–4455.
6. Joshi, R.K.; Kruis, F.E. Influence of Ag particle size on ethanol sensing of SnO_{1.8}: Ag nanoparticle films: A method to develop parts per billion level gas sensors. *Appl. Phys. Lett.* **2006**, *89*, 153116–153113.
7. Tricoli, A.; Graf, M.; Pratsinis, S.E. Optimal doping for enhanced SnO₂ sensitivity and thermal stability. *Adv. Funct. Mat.* **2008**, *18*, 1969–1976.
8. Carotta, M.C.; Ferroni, M.; Gnani, D.; Guidi, V.; Merli, M.; Martinelli, G.; Casale, M.C.; Notaro, M. Nanostructured pure and Nb-doped TiO₂ as thick film gas sensors for environmental monitoring. *Sens. Actuat. B Chem.* **1999**, *58*, 310–317.
9. Tricoli, A.; Righettoni, M.; Pratsinis, S.E. Minimal cross-sensitivity to humidity during ethanol detection by SnO₂-TiO₂ solid solutions. *Nanotechnology* **2009**, doi: 10.1088/0957-4484/20/31/315502.
10. Tricoli, A.; Righettoni, M.; Pratsinis, S.E. Anti-fogging nanofibrous SiO₂ and nanostructured SiO₂-TiO₂ films made by rapid flame deposition and *in situ* Annealing. *Langmuir* **2009**, *25*, 12578–12584.
11. Tricoli, A.; Righettoni, M.; Krumeich, F.; Stark, W.J.; Pratsinis, S.E. Scalable flame synthesis of SiO₂ nanowires: Dynamics of growth. *Nanotechnology* **2010**, doi: 10.1088/0957-4484/21/46/465604.
12. Kobata, A.; Kusakabe, K.; Morooka, S. Growth and transformation of TiO₂ crystallites in aerosol reactor. *AIChE J.* **1991**, *37*, 347–359.
13. O'Dell, L.A.; Savin, S.L.P.; Chadwick, A.V.; Smith, M.E. Structural studies of silica- and alumina-pinned nanocrystalline SnO₂. *Nanotechnology* **2005**, *16*, 1836–1843.

14. Savin, S.; Chadwick, A.V. Restricting the high-temperature growth of nanocrystalline tin oxide. *Radiat. Eff. Defects Solids* **2003**, *158*, 73–76.
15. Tricoli, A.; Graf, M.; Mayer, F.; Kühne, S.; Hierlemann, A.; Pratsinis, S.E. Micropatterning layers by flame aerosol deposition-annealing. *Adv. Mater.* **2008**, *20*, 3005–3010.
16. Bolzan, A.A.; Fong, C.; Kennedy, B.J.; Howard, C.J. Structural studies of rutile-type metal dioxides. *Acta Crystallogr. Sect. B Struct. Commun.* **1997**, *53*, 373–380.
17. Teleki, A.; Pratsinis, S.E.; Kalyanasundaram, K.; Gouma, P.I. Sensing of organic vapors by flame-made TiO₂ nanoparticles. *Sens. Actuat. B Chem.* **2006**, *119*, 683–690.
18. D'Amico, A.; di Natale, C. A contribution on some basic definitions of sensor properties. *IEEE Sens. J.* **2001**, *1*, 183–190.
19. Righettoni, M.; Tricoli, A.; Pratsinis, S.E. Thermally stable, silica-doped ε-WO₃ for sensing of acetone in the human breath. *Chem. Mat.* **2010**, *22*, 3152–3157.
20. Bittencourt, C.; Llobet, E.; Ivanov, P.; Correig, X.; Vilanova, X.; Brezmes, J.; Hubalek, J.; Malysz, K.; Pireaux, J.J.; Calderer, J. Influence of the doping method on the sensitivity of Pt-doped screen-printed SnO₂ sensors. *Sens. Actuat. B Chem.* **2004**, *97*, 67–73.
21. Keskinen, H.; Tricoli, A.; Marjamäki, M.; Mäkelä, J.M.; Pratsinis, S.E. Size-selected agglomerates of SnO₂ nanoparticles as gas sensors. *J. Appl. Phys.* **2009**, *106*, 084316:1–084316:8.
22. Barsan, N.; Weimar, U. Understanding the fundamental principles of metal oxide based gas sensors; the example of CO sensing with SnO₂ sensors in the presence of humidity. *J. Phys. Condes. Matter* **2003**, *15*, R813–R839.
23. Hahn, K.R.; Tricoli, A.; Santarossa, G.; Vargas, A.; Baiker, A. Theoretical study of the (110) surface of Sn_{1-x}Ti_xO₂ solid solutions with different distribution and content of Ti. *Surf. Sci.* **2011**, *605*, 1476–1482.
24. Hahn, K.R.; Tricoli, A.; Santarossa, G.; Vargas, A.; Baiker, A. First principles analysis of H₂O adsorption on the (110) surfaces of SnO₂, TiO₂ and their solid solutions. *Langmuir* **2011**, 1646–1656.
25. Vilaseca, M.; Coronas, J.; Cirera, A.; Cornet, A.; Morante, J.R.; Santamaria, J. Use of zeolite films to improve the selectivity of reactive gas sensors. *Catal. Today* **2003**, *82*, 179–185.
26. Vilaseca, M.; Coronas, J.; Cirera, A.; Cornet, A.; Morante, J.R.; Santamaria, J. Gas detection with SnO₂ sensors modified by zeolite films. *Sens. Actuat. B Chem.* **2007**, *124*, 99–110.
27. Righettoni, M.; Tricoli, A. Toward portable breath acetone analysis for diabetes detection. *J. Breath Res.* **2011**, doi: 10.1088/1752-7155/5/3/037109.